On the Consistency of EKF-SLAM: Focusing on the Observation Models

Amirhossein Tamjidi, Hamid D. Taghirad, *Member, IEEE*, Aliakbar Aghamohammadi, *Student Member, IEEE*

Abstract— In this paper a new strategy for handling the observation information of a bearing-range sensor throughout the filtering process of EKF-SLAM is proposed. This new strategy is advised based on a thorough consistency analysis and aims to improve the process consistency while reducing the computational cost. At first, three different possible observation models are introduced for the EKF-SLAM solution for a robot equipped with a bearing-range sensor. General form of the covariance matrix and the level of inconsistency in the robot orientation estimate is then calculated for these variants, and based on the numerical comparison of the estimation results, it is proposed to use the bearing and range information of a feature in the initialization step of EKF-SLAM. However, it is recommended to use only the bearing information to perform other iteration steps. The simulation observations verify that the new strategy yields to more consistent estimates both for the robot and the features. Moreover, through the proposed consistency analysis, it is shown that since the source of consistency improvement is independent from the choice of the motion model, it gives us an advantage over other existing methods that assume a specific motion models for consistency improvement.

Index Terms— Consistency Analysis , EKF-SLAM, Observation Model

I. Introduction

THE problem of Simultaneous Localization and Mapping (SLAM) has been an active research area for last two decades and Extended Kalman Filter (EKF) based approaches to the SLAM problem are among the most popular algorithms developed so far. EKF-SLAM involves building a map of features while computing a robot's trajectory through that map based on noisy sensor and actuator data. According to the standard EKF algorithm, motion and observation models are being linearized around the latest available estimate of the system state vector by Taylor expansion. This process could greatly affect the performance of the filter which is generally analyzed by convergence and consistency.

Early convergence proofs of EKF-SLAM algorithm assumed that the observation and motion models to be linear [1]. Most of these convergence properties still hold true for the nonlinear case provided that the Jacobians are evaluated at the true state of the system [2]. Such an assumption is generally violated in real world situations and could make the solution of the EKF-SLAM inconsistent. One of the first researches on filter inconsistency in EKF-based SLAM was

discussed in [3], and it is shown that in a stationary robot with no process noise, by measuring the relative position of a new landmark multiple times, the estimated variance of the robot orientation decreases unexpectedly. It is further shown that this is due to the violation of a fundamental relationship between different system Jacobians. Since then, significant empirical evidence of filter inconsistency in moving robot scenarios has been reported in several works [4], [5], [6] which in turn has drawn researcher's attention to ponder its roots in more detail and devise new methods to improve filter consistency. Research efforts in this area fall into two categories: those that aim at reducing the robot state uncertainty and consequently linearization errors [5], [7], and those based on observability analysis [8], [9], [10].

In [5] based on extensive simulation studies, it is suggested that in order to improve consistency, the uncertainty of the robot orientation should be kept small enough by making regular observations of the robot heading. In [7] consistency improvement is achieved using a robot centered representation of the environment and a modified filtering approach both of which aim to reduce the uncertainty of the robot state.

An example of consistency improvement through observability analysis is given in [10], in which anchoring the map to the first seen observation or using an external sensor like GPS is proposed. However, this approach is bounded to a set of assumptions and could not be applied in general. Recently, Huang et al. in [8], [9] presented an observability based study of the inconsistency problem in EKF-SLAM and proposed a new filtering strategy based on First Estimate Jacobians and is called FEJ-EKF. According to this analysis, as a result of evaluating Jacobians at the latest state estimates rather than the true states, the unobservable subspace of the standard EKF-SLAM does not match that of the ideal EKF-SLAM. Consequently, the estimated orientation covariance is mistakenly reduced when actually no information is injected to the system, and this causes inconsistency. FEJ-EKF attempts to preserve the rank of the linearized error-state system the same as the rank of the underlying nonlinear system and this is achieved by evaluating the filter Jacobians at the first-ever available estimates for each state variable.

In this paper, we concentrate on the role of observation model on the consistency improvement. The concept of measuring the relative bearing and range of a point in the environment is shared in modeling of most exteroceptive sensors mounted on mobile robots. Therefore, devising a general strategy for handling such information throughout the filtering procedure with the goal of consistency improvement

A. Tamjidi and H. D. Taghirad are with Electrical Engineering Department, K.N. Toosi University of Technology, Tehran, Iran. Email: ahtamjidi@ee.kntu.ac.ir and taghirad@kntu.ac.ir.

A. Aghamohammadi is with Computer Science and Engineering Department, Texas A&M University, College Station, TX, 77843. Email: ali@cse.tamu.edu.

could have a broad application. It is desired that such an strategy does not require additional computational cost or sensor and does not rely on the kinematic model of the robot, otherwise it would impose a constraint on applicability of the method.

II. PROBLEM FORMULATION

Consider a mobile robot moving in a 2D environment and equipped with a bearing-range sensor such as Laser Range Finder (LRF). From the observation model point of view, one can assume three different models as the observation model for EKF-SLAM: Bearing-Range observation model (BR), Bearing-Only observation model (BO) and Range-Only observation model (RO). Adopting each of these observation models results in a variant of EKF-SLAM, which as it will be shown later, exhibits a different filter performance from the consistency perspective. In the following we will discuss these variants in more details.

Representing the state vector in Gaussian form, the goal of a typical EKF-SLAM solution is to use the information obtained from the observation and motion model of a mobile robot in order to estimate the mean and covariance matrix of the augmented vector of robot state, X_v^T, and stacked state vector of stationary features in the environment, X_f^T. We will denote the augmented vector $X = [X_v^T, X_f^T]^T$ as *system state vector*. The robot state vector $X_v^T = [x_v, y_v.\theta_v]$ represents the robot position and orientation in a reference coordinate frame and the features state vector $X_f = [f_1^T, f_2^T, \cdots, f_n^T]^T$ consists of individual feature coordinates in the same reference coordinate frame. In the beginning of the EKF-SLAM process the system state vector is comprised only of the robot state vector and is generally initialized to zero. Three aforementioned variants have a similar outline for implementation and hence are summarized in the following collectively.

A. Prediction

State Prediction: In this stage, robot control inputs are processed to obtain a prediction for robot state and the covariance of the system state is propagated through the linearized motion model. For clarity and brevity purposes, $'+'$ and $'-'$ superscript are used to identify the state vector and covariance matrix values after update and after prediction stages, respectively. General motion model for system state vector becomes:

$$X^-(k) = f\left(X^+(k-1), \mathbf{u_k}\right), \qquad (1)$$

in which, $\mathbf{u_k}$ is the control input with zero mean Gaussian noise with covariance Q, $\mathbf{n} \to N(0, Q)$ and $f(\cdot)$ is the function, which describes system state vector's dynamics. In prediction step, $P^-(k)$ which is the covariance matrix of prediction for system state vector is also calculated using covariance propagation equations in linear systems.

Observation Prediction: Having the results of the previous step at hand and knowing the type of the observation model as well as the sensor field of view, one can readily determine whether a feature is seen at the current step and can predict

its corresponding measurement as well. As mentioned before, we assume that the robot is equipped with a bearing-range sensor which enables it to measure the relative position of a feature with respect to the robot. Therefore, without any restriction one can assume the range or bearing part or both of them as the sensor measurement. Advantages and disadvantages of each alternative will be discussed later in the next section.

For a feature $f = (x_f, y_f)^T$ in the reference coordinate the bearing-range observation model is as follows:

$$\begin{pmatrix} r_f \\ \phi_f \end{pmatrix} = \begin{pmatrix} \sqrt{(x_f - x_v)^2 + (y_f - y_v)^2} \\ \arctan(\frac{y_f - y_v}{x_f - x_v}) - \theta_v \end{pmatrix}. \qquad (2)$$

Let us denote the bearing-range, range-only and bearing-only observation models by $h^{BR}(X) = (r_f, \phi_f)$, $h^{RO}(X) = r_f$ and $h^{BO}(X) = \phi_f$, respectively. At the current step, some features are extracted from the senor's raw data. In practice, observed features are fed into a data association procedure to find out possible correspondence between previously seen features and currently observed ones. After this step, observed features fall into two categories: newly observed features and previously seen features. The former is stored to be augmented to the system state vector in augmentation step and the later will be used in updating step. No matter what kind of observation model is used, the corresponding measurement prediction vector $Z^-(k)$ for the features in the second category can be calculated as the stacked vector of the individual sensor measurement predictions $z_i^-(k)$. For bearing-range observation model, observation Jacobian for the $H_i^{RB} = \partial h^{BR} / \partial X|_{(f_i^-, X_v^-)}$ is calculated by substituting (f_i^-, X_v^-) in the following equation in which $r = r_f$, $\phi = \phi_f$, $c_\phi = cos(\phi)$ and $s_\phi = sin(\phi)$.

$$H^{BR} = \begin{pmatrix} -c_\phi & -s_\phi & 0 & c_\phi & s_\phi \\ \frac{s_\phi}{r} & \frac{-c_\phi}{r} & -1 & \frac{-s_\phi}{r} & \frac{c_\phi}{r} \end{pmatrix}. \qquad (3)$$

For the bearing-only and range-only case H_i^{BO} and H_i^{RO} are composed of the first and second rows of the H_i^{BR} in 3, respectively. Overall observation Jacobian matrix H is obtained by stacking up H_i^{BR}'s or H_i^{BO}'s or H_i^{RO}'s depending on the adopted observation model.

B. Update & Augmentation

Update: Supposing R to be the observation covariance matrix, covariance update rule can be expressed in information form.

$$\Omega^-(k) = P^-(k)^{-1} \qquad (4a)$$
$$\Omega^+(k) = \Omega^-(k) + \Omega_{new}(k) \qquad (4b)$$
$$P^+(k) = \Omega^+(k)^{-1}, \qquad (4c)$$

where, $\Omega(\cdot)$ is the information matrix, $\Omega_{new}(k) = H(k)R^{-1}(k)H(k)^T$ is the new information obtained from the sensor measurement. Information form of EKF update will be used in the next section, where we analyze the amount of inconsistency incurred in the filtering process.

Augmentation: In this stage, first-ever seen features are included in the system state vector through the inverse

observation model and the covariance matrix of the system state vector is expanded in order to include the new correlation information corresponding to the newly observed features and the remaining part of the system state vector. More accurate a feature is initialized into the system state vector, more consistent the filter will perform. Therefore, contrary to the observation step, for all three variants we use the inverse function of the bearing-range observation model $g(X_v, r_f, \phi_f)$ for feature initialization.

III. CONSISTENCY ANALYSIS

Under the Linear-Gaussian assumption the pair (x^+, P^+), is a consistent estimate for two first statistical moments of the random variable x if the two following conditions are satisfied:

$$E[x - x^+] = 0 \quad (5a)$$
$$E[(x - x^+)(x - x^+)^T] = 0. \quad (5b)$$

So far, analytical results for EKF-SLAM consistency evaluation have considered the cases of a stationary robot making n observations of a feature from one or two poses. The former case in which robot observes a feature from one pose is of interest since the effect of observation model on the extent of inconsistency could be calculated for it. For a robot with initial uncertainty P_0 observing a feature n times with covariance R, if all Jacobians are calculated at the true state, according to Theorem 3.2 in [2] the general expression for covariance matrix of the augmented system state vector becomes:

$$P^+(n) = \begin{pmatrix} P_0 & P_0 A_e^T \\ A_e P_0 & A_e P_0 A_e^T + \frac{A^{-1} R A^{-T}}{n} \end{pmatrix}, \quad (6)$$

where, matrices A_e and A are obtained from the Jacobians of the BR observation model. Calculation of the general form of the $P^+(n)$ matrix of other variants is not as straightforward as the BR case, since the final information matrix becomes non-invertible after n observations. In such case inversion lemma, which is used in [2] could not be applied. However, it is clear that since the sensor always measures the relative position of the feature with respect to the robot, for a stationary robot, observing a single feature n times, the robot state vector and its covariance should remain unchanged irrespective of the choice of the observation model. Deviation from this ideal covariance is a symptom of inconsistency and the extent of this deviation determines the level of inconsistency in covariance matching. It can be shown that if all Jacobians are calculated at the true state, the covariance matching condition for the robot state is preserved. However, in real world such an assumption is violated since we do not know the true state of a feature and due to noisy observations, at each time instant the Jacobians are calculated at a different feature state. Therefore, it is expected that the estimated covariance will not match the real one.

Another point to be considered in performance evaluation is the amount of error in the process of state estimation. According to (5a) being unbiased is also an important issue in filter consistency. Therefore, both conditions of covariance matching and being unbiased should be met in order for an estimate to be called completely consistent.

In the following we first analyze mathematically the covariance matching condition for the robot orientation uncertainty for all the three EKF-SLAM variants. Then we use a graphical tool to visualize the effect of the observation model on covariance estimation. Further numerical analysis that examines both unbiasedness and covariance matching conditions for estimation in stationary and moving robot scenarios will be considered in section IV.

Suppose a robot with initial state vector $X_v = [0, 0, 0]^T$ and a diagonal initial covariance $P_0 = diag(\sigma_x, \sigma_y, \sigma_\theta)$ and initial information matrix $\Omega_0 = P_0^{-1}$. The robot is stationary with no process noise and observes a feature f for n times with covariance R. As mentioned earlier regardless of the variant of the EKF being used, inverse BR observation model is employed for feature augmentation. In information form, such augmentation is realized by adding $\left(H_i^{BR}\right)^T (R^{BR})^{-1} H_i^{BR}$ to the robot initial information matrix. Here H_i^{BR} is the Jacobian of the BR observation model when observing the feature for the first time and $R^{BR} = diag(\sigma_r, \sigma_\phi)$ is the corresponding observation covariance matrix. After the first step, each variant of EKF will have a different information matrix and consequently different covariance matrix. Assuming H_i to be the observation model Jacobian (either BR, BO or RO) in step i and R to be the relevant observation covariance the final information matrix of the system after n observations for $n > 1$ is:

$$\Omega_n = \begin{pmatrix} \Omega_0 & 0_{3 \times 2} \\ 0_{2 \times 3} & 0_{2 \times 2} \end{pmatrix} + (H_1^{BR})^T (R^{BR})^{-1} H_1^{BR} \quad (7)$$
$$+ \sum_{i=2}^{n} H_i^T R^{-1} H_i,$$

and the final covariance matrix is $P_n = \Omega_n^{-1}$. In all variants of EKF, P_n has the following general form:

$$P_n = \begin{pmatrix} \sigma_x & 0 & 0 & \sigma_x & 0 \\ 0 & \sigma_y & 0 & 0 & \sigma_y \\ 0 & 0 & \gamma(n)\sigma_\theta & \omega_{34} & \omega_{35} \\ \sigma_x & 0 & \omega_{43} & \omega_{44} & \omega_{45} \\ 0 & \sigma_y & \omega_{53} & \omega_{54} & \omega_{55} \end{pmatrix}, \quad (8)$$

in which, $\omega_{ij}(n)$'s and $\gamma(n)$ are determined based on the employed observation model and observation step. In addition, as it will be shown in all variants of EKF, $\gamma(n)$ has the following general form:

$$\gamma(n) = \frac{\Psi(n)}{\Psi(n) + \Upsilon(n)}, \quad (9)$$

where, $\Psi(n)$ and $\Upsilon(n)$ are function of robot observations up to step n and $\{\sigma_r, \sigma_\phi, \sigma_\theta\}$. Ideally, $\gamma(n)$ is expected to be equal to one in order for the covariance matching condition of (5b) to be met. Therefore, the mathematical analysis of this coefficient in three EKF variants is of interest. In the following r_i and ϕ_i are sensor observations in step i and $s_{(\cdot)} = sin(\cdot)$ and $c_{(\cdot)} = cos(\cdot)$.

Bearing-Only: for $n = 2$ we have

$$\Psi^{BO}(2) = s_{\phi_1-\phi_2}^2 \sigma_r + (\tfrac{1}{2} r_2^2 + r_1^2 c_{\phi_1-\phi_2}^2)\sigma_\phi \quad (10)$$
$$\Omega^{BO}(2) = (r_2 - r_1 c_{\phi_1-\phi_2})^2 \sigma_\theta.$$

Range-Only: for $n = 2$ we have

$$\Psi^{RO}(2) = r_1^2 s_{\phi_1-\phi_2}^2 \sigma_\phi + (1 + c_{\phi_1-\phi_2}^2)\sigma_r \quad (11)$$
$$\Omega^{RO}(2) = r_1^2 s_{\phi_1-\phi_2}^2 \sigma_\theta.$$

Bearing-Range: for $n = 2$ we have

$$\Psi^{BR}(2) = r_1^2 r_2^2 s_{\phi_1-\phi_2}^2 \sigma_\phi^2 \quad (12)$$
$$+ (r_1^2 + r_2^2)(1 + c_{\phi_1-\phi_2}^2)\sigma_\phi\sigma_r + s_{\phi_1-\phi_2}^2 \sigma_r^2$$
$$\Omega^{BR}(2) = \big(2(r_1^2 + r_2^2)(1 + c_{\phi_1-\phi_2}^2) - 4r_1 r_2 c_{\phi_1-\phi_2}\big)\sigma_r\sigma_\theta$$
$$+ 2r_1^2 r_2^2 s_{\phi_1-\phi_2}^2 \sigma_\phi\sigma_\theta$$

These expressions are calculated and simplified using Matlab and Mathematica. Expressions of $\gamma(n)$ for different steps are also calculated which confirm below claims about the behavior of this coefficient in different EKF variants. Close inspection of Ψ's and Ω's in above equations reveals two facts: first, that for all three variants of EKF, $\gamma(n)$ has a radial symmetry and the value of $\gamma(n)$ depends on the noise of the bearing observation rather than bearing observation itself; second, that the stochastic nature of the sensor observations makes it difficult to perform any deterministic calculation on the amount of inconsistency introduced by $\gamma(n)$ in estimation process. As a result an appropriate numerical method should be devised in order to make comparison between EKF variants.

To facilitate the numerical analysis and to visualize the effect of $\gamma(n)$ on uncertainty reduction we propose to use a graphical diagram, which we will refer to it as "consistency map". In order to produce such a graph, suppose that the robot is located in the center of a square with side length of 50m. Divide this square into 0.5m×0.5m grid cells and calculate $\gamma(n)$ at the center of each cell. Plot the results in a 2-dimensional graphical-map encoding the $\gamma(n)$ value as a color-point. The greater is the area of the consistency map in which $\gamma(n)$ is close to one, the greater is the area in which covariance matching condition is met and consequently the better is the performance of the filter.

Example plots of consistency map for the BO, RO and BR variants of the EKF-SLAM are shown in Fig. 1, 2 and 3, respectively. In producing these figures, the value of $\gamma(n)$ is calculated after 10 observations ($n = 10$) and sensor parameters σ_θ and σ_r are set to $(0.5°)^2$ and 0.1^2, respectively. It is evident from the consistency maps of EKF variants that the BO variant outperforms two others, in covariance matching sense, because $\gamma(n)$ is mostly equal to one in the BO consistency map except for a small area in center of the map. Fig. 2 shows that for features that are too close to the robot the RO variant outperforms two other variants but in other areas it has a similar performance to the BR variant. Finally, Fig. 3 illustrates that in most of the areas around the robot the BR variant has a poor performance in covariance matching sense.
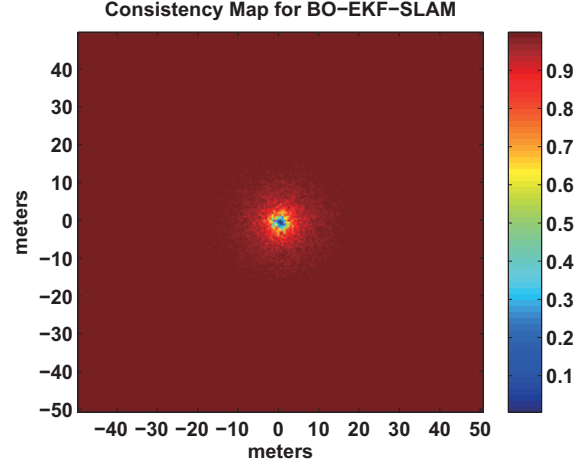

Fig. 1. Consistency map for the BO EKF-SLAM. $\gamma(10)$ is mostly equal to one for most of the features except for those located in a small area near the center of the map.
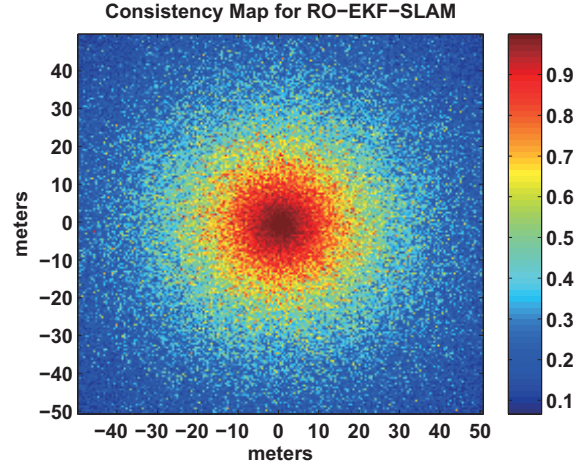

Fig. 2. Consistency map for the RO EKF-SLAM. $\gamma(10)$ is mostly close to zero in the RO consistency map, especially for features located in distant areas from the robot.
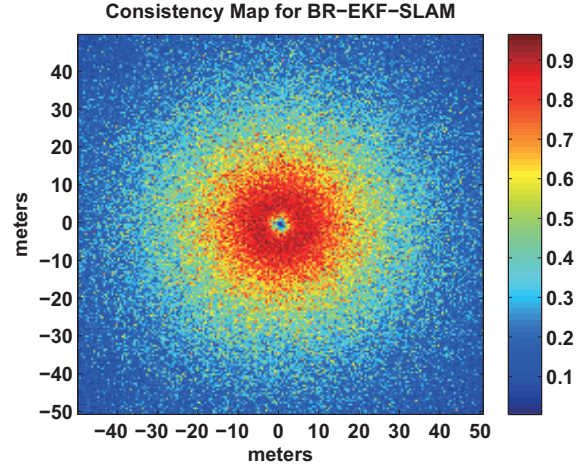

Fig. 3. Consistency map for the BR EKF-SLAM. $\gamma(10)$ is mostly close to zero in the BR consistency map, especially for features located in distant areas and a small area near the center of the map.

IV. SIMULATION RESULTS

In order to test both conditions of filter consistency for three EKF variants introduced so far, in this section we consider two other cases: first a stationary robot observing

a single landmark, second a moving robot which tracks a closed path twice. For sake of comparison, in stationary robot scenario, simulation conditions are adopted from [3] and in moving robot scenario the environment and sensor parameters are selected as in [5]. The stationary robot scenario is of great importance as the ideal covariance for the system state vector can be calculated for it before the simulation is executed, and this allows us to determine the performance of the filter in a measurable manner. Furthermore, the simplicity of the scenario makes it easier to scrutinize the effect of the sensor model or the location of the feature on the estimation process.

However, in practice, many parameters can affect the performance of the filter and the effect of most of them has not been analyzed yet. For example, it has not been explained yet in what way the geometry of the features map and the path of the robot can affect the performance of the filter. This necessitates testing any devised filtering strategy on moving robot scenarios where the ground truth is available to see whether the filter preserves its positive characteristics in real experiments.

a) Stationary Robot: To examine the behavior of the estimation error we simulate the stationary robot scenario for the BR and BO variants with exactly the same set of noisy observations. In this simulation the robot is supposed to be stationary at point $[0, 0]$ with no process noise. The initial covariance of the robot state vector is considered as $P_0 = diag(0.7^2, 0.7^2, (0.5°)^2)$ and it is assumed that there is only one feature at point $[70.1, 97.89]$ and the robot observes it for 500 consecutive steps. The sensor parameters σ_θ and σ_r are set to $(0.5°)^2$ and 0.1^2, respectively.

Figures 4, 5 and 6 illustrate the time history of the estimation errors as well as the estimated and ideal 2σ covariance bounds of robot orientation, and feature state components for the BO, BR and RO variants, respectively. For the feature, ideal 2σ covariance bounds are obtained by calculating Jacobians at true state vector. Also, for robot orientation, it is expected that estimated 2σ covariance bounds remain unchanged and any increase and decrease is a sign of inconsistency.

From the consistency map of BO-EKF in Fig. 2 one can expect that BO-EKF would outperform two other variants in covariance matching sense. Fig. 6 shows that the BO variant not only has the best performance in covariance matching sense but also has the lowest amount of estimation error among other variants. On the other hand, Fig. 5 demonstrates that in case of using BR-EKF the covariance estimate of the robot orientation starts to decline immediately after the first observation, as expected, and then approximately bottoms out at 20th time step. Feature covariance estimates undergo a similar decline and these spurious updates in turn create a bias in estimation error for the feature state as well as the robot orientation. Fig. 6 shows that inconsistency also occurs in RO-EKF. Estimated uncertainty bounds start to decline after step 179 when simultaneously a peak is appeared in estimation errors.
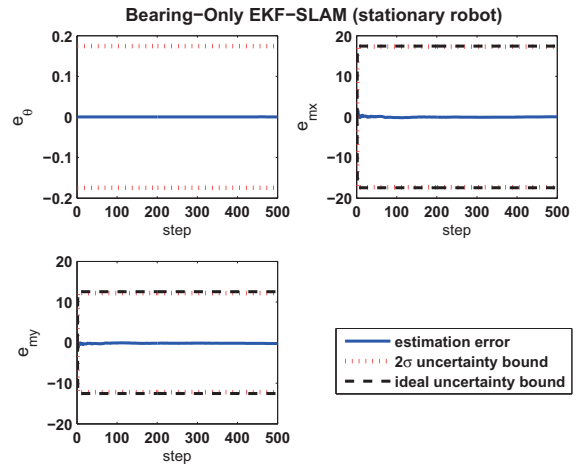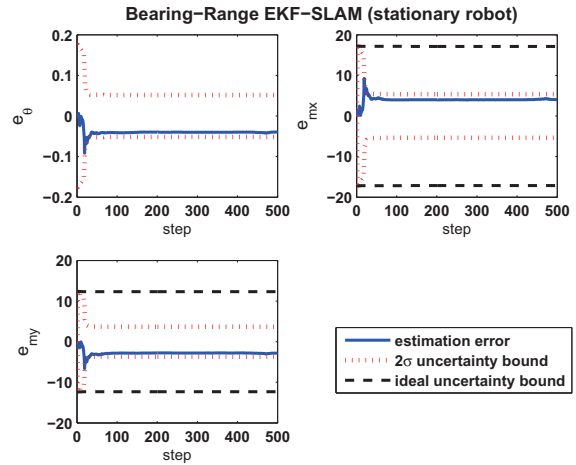

Fig. 4. Estimation error behavior in the stationary robot scenario using BO-EKF-SLAM. Maximum estimation error for feature's x and y coordinates are $e_{mx} = 1.52m$ and $e_{my} = -1.25m$, which both occur at 3rd time step. Ideal 2σ uncertainty bound is obtained by calculating Jacobians at true state vector. Estimated and ideal covariances are nearly identical.
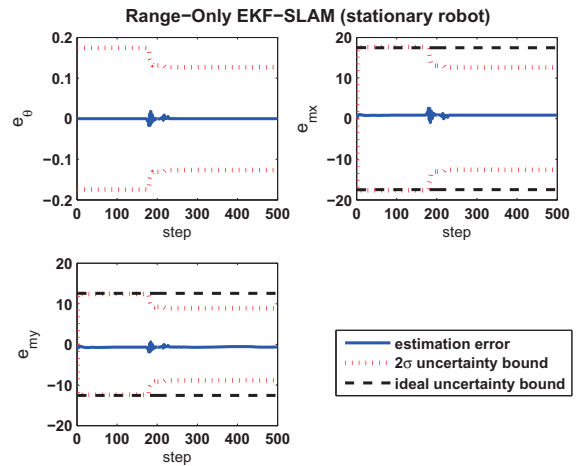

Fig. 5. Estimation error behavior in the stationary robot scenario using BR-EKF-SLAM. Maximum estimation error for feature's x and y coordinates are $e_{mx} = 9.27m$ and $e_{my} = -6.63m$, which both occur at 19th time step. Ideal 2σ uncertainty bound is obtained by calculating Jacobians at true state vector. Estimated and ideal covariances do not match.

Fig. 6. Estimation error behavior in the stationary robot scenario using RO-EKF-SLAM. Maximum estimation error for feature's x and y coordinates are $e_{mx} = 2.58m$ and $e_{my} = -1.87m$, which both occur at 179th time step. Ideal 2σ uncertainty bound is obtained by calculating Jacobians at true state vector. Estimated and ideal covariances do not match.

b) Moving Robot (Simulation): In this simulation, the moving robot scenario of [5] is considered. The scenario is run for BR, BO and RO variants of EKF-SLAM over 50 Monte Carlo simulations. The average Normalized (state) Estimation Error Squared (NEES) results for the robot state estimates and three example feature estimates are shown in Fig. 7 and Fig. 8, respectively. As it can be seen in these figures, by applying the BO observation model, not only the robot state estimates become more consistent but also the upper bounds of the average NEES [11] for the features in the map is significantly decreased and the estimations of the features' states are closer to consistency compared to that of other variants. Although the traditional EKF-SLAM outperforms BO-EKF-SLAM for a few steps, generally its average NEES is above the average NEES of the BO case, which is an indication of its overall inferiority.

Interestingly, the RO observation model yields to the worst results after closing the loop. Comparing this with the results of the BO-EKF shows that although RO-EKF has a similar performance in the first loop, it fails to appropriately close the loop and therefore loses its consistency.
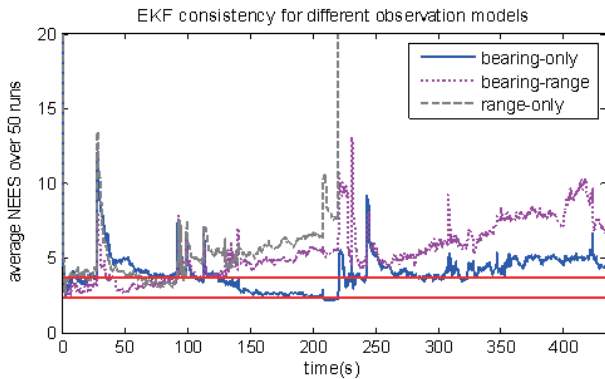

Fig. 7. Average NEES for the robot pose estimate over 50 Monte Carlo simulations for three EKF variants. The horizontal lines mark the 95% probability concentration region for a 3-dimensional state vector. The bearing-only variant remains in the boundary for the longest time steps.
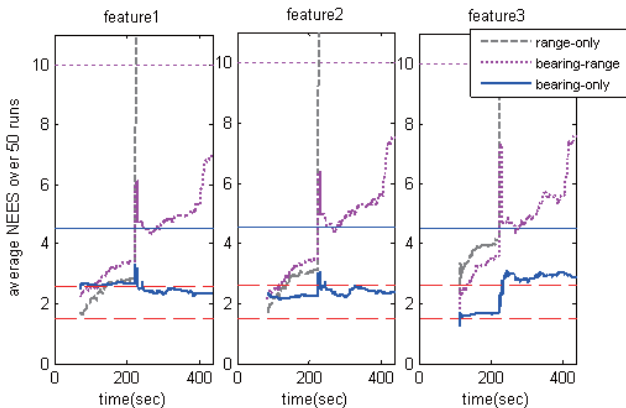

Fig. 8. Average NEES of typical features' estimate over 50 Monte Carlo simulations for three EKF variants. The horizontal dashed lines mark the 95% probability concentration region for a 3-dimensional state vector. The horizontal solid and dotted lines show the maximum average NEES of all the features.

V. CONCLUSIONS

In this paper we have analyzed the role of the observation model on the filter performance in the EKF-SLAM problem.

Supposing that the robot is equipped with a Bearing-Range sensor such as LRF, we considered three different possible strategies for sensor information handling in the filtering procedure. For each strategy we calculated the general form of the system covariance matrix in the simple and mathematically tractable scenario of a stationary robot n times observing a single landmark. This allowed us to separate the effect of the choice of the observation model from the effect of the motion model on inconsistency. The use of a graphical tool termed as consistency map made it possible to visualize and compare the extent of inconsistency of different strategies in the filtering procedure. It is emphasized that for filter consistency both conditions of unbiasedness and covariance matching should meet in stationary and moving robot scenarios. The case of RO observation model is represented as an example that satisfies both conditions in stationary robot scenario but exhibits severe inconsistency in moving robot scenario.

The analysis of the stationary robot scenario indicated that BO observation model might also lead to consistency improvement, a hypothesis that is corroborated by simulation results for moving robot scenario. In fact, simulations showed that using BO observation model not only the level of inconsistency in robot state estimation is reduced, but also the average NEES bounds for features' states are clearly reduced.

REFERENCES

[1] M. Dissanayake, P. Newman, S. Clark, H. Durrant-Whyte, and M. Csorba, "A solution to the simultaneous localization and map building (SLAM) problem," *IEEE Transactions on Robotics and Automation*, vol. 17, no. 3, pp. 229–241, 2001.

[2] S. Huang and G. Dissanayake, "Convergence and consistency analysis for extended Kalman filter based SLAM," *IEEE Transactions on Robotics*, vol. 23, no. 5, pp. 1036–1049, 2007.

[3] S. Julier and J. Uhlmann, "A counter example to the theory of simultaneous localization and map building," in *IEEE International Conference on Robotics and Automation*, vol. 4, pp. 4238–4243, 2001.

[4] A. Castellanos, J. Neira, and J. Tardos., "Limits to the consistency of ekf-based slam," in *IFAC Symposium on Intelligent Autonomous Vehicles*, 2004.

[5] T. Bailey, J. Nieto, J. Guivant, M. Stevens, and E. Nebot, "Consistency of the EKF-SLAM algorithm," in *2006 IEEE/RSJ International Conference on Intelligent Robots and Systems*, pp. 3562–3568, 2006.

[6] U. Frese, "A discussion of simultaneous localization and mapping," *Autonomous Robots*, vol. 20, no. 1, pp. 25–42, 2006.

[7] J. Castellanos, R. Martinez-Cantin, J. Tardos, and J. Neira, "Robocentric map joining: Improving the consistency of EKF-SLAM," *Robotics and Autonomous Systems*, vol. 55, no. 1, pp. 21–29, 2007.

[8] G. Huang, A. Mourikis, and S. Roumeliotis, "Analysis and improvement of the consistency of extended Kalman filter based SLAM," in *IEEE International Conference on Robotics and Automation, 2008. ICRA 2008*, pp. 473–479, 2008.

[9] G. Huang, A. Mourikis, and S. Roumeliotis, "Analysis and improvement of the consistency of extended kalman filter based slam," tech. rep., University of Minnesota, Minneapolis, MN, August 2007.

[10] J. Andrade-Cetto and A. Sanfeliu, "The effects of partial observability when building fully correlated maps," *IEEE Transactions on Robotics*, vol. 21, no. 4, pp. 771–777, 2005.

[11] Y. Bar-Shalom, X. Li, and T. Kirubarajan, *Estimation with applications to tracking and navigation*. Wiley New York, 2001.